2010 IEEE International Conference on Robotics and Automation
Anchorage Convention District
May 3-8, 2010, Anchorage, Alaska, USA

Design and Control of an Underactuated Three-Link Rolling Biped

Louis L. Flynn, Rouhollah Jafari and Ranjan Mukherjee

Abstract— **We present the design and control of a simple three-link underactuated synthetic wheel biped composed of a torso and two legs with arc-shaped feet. The equations of motion are derived and a controller based on feedback linearization is used to constrain the controllable degrees of freedom and develop a simple gait. Experimental results show successful gait generation and relatively good trajectory tracking. The data on energy consumption indicates a reasonably low cost of transport, even without design or trajectory optimization.**

I. INTRODUCTION

The study of bipeds began at Waseda University with the development of the statically stable WL-1 in 1967. Later developments at Waseda led to the first quasi-dynamic (WL-9DR) and completely dynamic (WL-10DR) bipeds [1]. The completely dynamic biped [2] employs high-gain controllers to track trajectories satisfying the ZMP[1] condition, developed by Vukobratovic and Juricic [3]. The ZMP method and its different interpretations [3], [4], [5], [6] has led to the development of the most stable biped platforms to date [7], [8], [9] including the ASIMO line of robots from Honda and its clones [10], [11].

Many bipeds, such as the Rabbit [12], do not follow the ZMP criterion for stability. Rabbit is controlled using the virtual constraint and hybrid zero dynamics method [13] which creates a single DOF[2] system by applying virtual constraints. The ankle joint of Rabbit is passive and all other joints are controlled to follow trajectories strictly based on the angle of the ankle. Any locomotion gait involves synchronous movement of relevant DOFs of the system and in this regard the synthetic wheel biped, presented in this paper, has similarities with Rabbit.

Impedance control has been implemented in a number of biped platforms [14], [15]. Many bipeds have also been developed with compliant linkages with the intention of exploiting the natural dynamics of the system during some portion of the gait cycle such as the hopping robots by Raibert [16], and the biped by Pratt [17]. The desire for compliance also led to the development of WL-14 [18] and Lucy [19] that incorporate variable stiffness in their drives with the intention of reducing energy consumption.

Passive Dynamic Walkers (PDW's) are the most energy-efficient walking machines requiring no actuation to find stable gaits, although they suffer from sensitivity to initial conditions and lack robustness to disturbances. McGeer [20] developed a kneed PDW that can walk down slopes with a periodic gait without feedback control. The disturbance response of PDW's was investigated by McGeer [20] using limit cycle analysis and by Hobbelen, et al. [21] using the concept of gait sensitivity norm. These concepts have been used to develop several energy-efficient bipeds with varying number of actuated joints and passive DOFs [22], [23], fixed point generation through kinematic constraints [24], as well as the effect of an upper body [25].

In this paper we propose the design for a new biped robot. Based on the concept of a self-propelled wheel [26], our biped promises to provide impact-free motion during walking. The conceptual design of the biped is provided in section II. The mathematical model is developed in section III: the equations of motion are derived and a gait is developed by imposing constraints. In section IV we present a simple control design for imposing the constraints and generating the gait. Experimental results are presented in section V and Section VI provides concluding remarks.

II. CONCEPTUAL DESIGN

The biped robot design presented in this paper is based on the concept of a self-propelled wheel, proposed earlier by Das and Mukherjee [26]. The self-propelled wheel, shown in Fig.1(a), has three eccentric masses that are constrained to move along radial spokes 120 degrees apart. The unbalance of these masses drive the wheel. The mass unbalance can also be created by continuously changing the relative angular position of the spokes while keeping the radial distance of the masses fixed, as shown in Fig.1(b). Our biped robot design is derived from the design in Fig.1(b) by replacing the three spokes with unbalance masses with two legs and a torso. In our design, shown in Fig.1(c), arc-shaped feet are used to eliminate the need for a continuous rim.

To understand the principle of operation of the biped in Fig.1(c), consider the scenario where the legs are constrained to remain symmetric with respect to the vertical and the torso maintains some fixed angle with the vertical. With the legs always symmetric with respect to the vertical, the moment due to the weight of the torso will cause the biped to roll over the stance leg. As the point of contact with the ground reaches the toe of the stance leg, the swing leg will have positioned itself in front of the stance leg such that the point of contact with the ground can smoothly transition from the toe of the stance leg to the heel of the swing leg. After the transition, the swing leg will become the stance leg and vice versa, and the biped will have completed one step of walking. To move in the backward direction, the torso will simply lean

All authors are with the Department of Mechanical Engineering, Michigan State University, East Lansing, MI, 48824, USA. The corresponding author is R. Mukherjee, email: mukherji@egr.msu.edu

[1]Zero Moment Point

[2]Degree-Of-Freedom

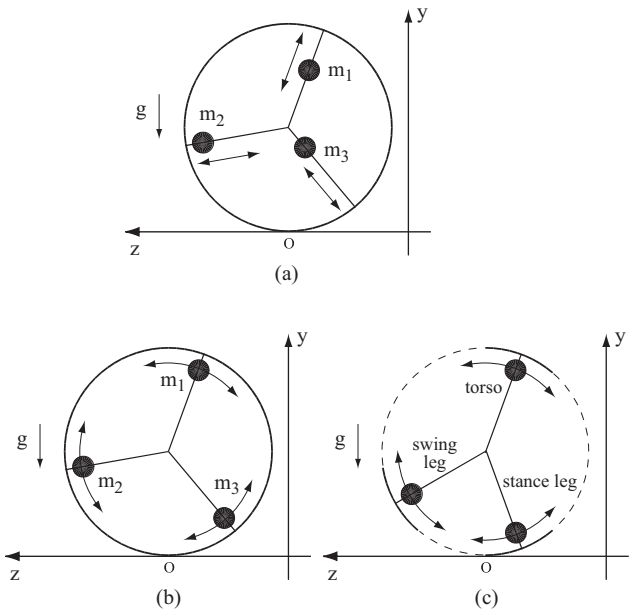

Fig. 1. (a) A self-propelled wheel using unbalance masses, (b) Design variant of the self-propelled wheel, (c) Conceptual design of biped with torso

backwards. This will cause the biped to slow down, if it was moving forward, and eventually reverse direction.

Through proper control design, the biped will avoid impact with the ground during support leg switching. This will eliminate the necessity for modeling collision dynamics which, together with a low number of degrees of freedom, simplifies the analysis. Our biped design in Fig.1(c) does not have a complete rim like the wheels in Figs.1(a) and (b). The functionality of the wheel is, however, maintained by proper placement of the swing leg and hence the descriptor *synthetic wheel*.

It is assumed that each leg of the biped will have a prismatic joint - this will enable the legs to contract in length and avoid contact with the ground during the swing phase while having a limited effect on the dynamics of the system, allowing us to further simplify the analysis by ignoring the dynamics of the prismatic joints. The design should also require very little energy input; ideally a robot of this design could have zero energy consumption as discussed in [20], although this has not been a focus of the current design. A robot of this type could also walk both forward and backward with little to no change of the controller due to its symmetric design. Due to these qualities, we feel that the synthetic wheel design is a good test bed for our controller and a starting point for our future work in biped design. In the next section we present the dynamic model of the biped.

III. MATHEMATICAL MODEL

A schematic of the synthetic wheel biped is shown in Fig.2. It has three DOFs and can be described by the generalized coordinates: θ, ψ and ϕ. These angles denote the angle of the stance leg with respect to the vertical, the angle of the swing leg with respect to the stance leg, and angle of the torso with respect to the stance leg, respectively. The biped has two actuators corresponding to the generalized coordinates ψ and ϕ and represents an under-actuated system.

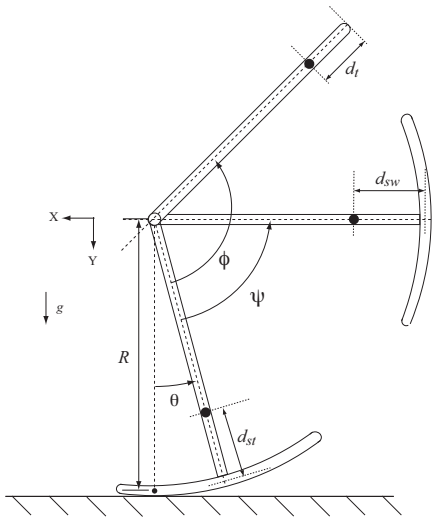

Fig. 2. A schematic of the synthetic wheel biped

Using Lagrange's equations, the dynamics of the system can be written in the form

$$M(q)\,\ddot{q} + N(q,\dot{q})\,\dot{q} + G(q) = T \tag{1}$$

where q is the vector of generalized coordinates and T is the vector of generalized forces, given by the relations

$$q = \begin{bmatrix} \theta \\ \phi \\ \psi \end{bmatrix}, \qquad T = \begin{bmatrix} 0 \\ \tau_1 \\ \tau_2 \end{bmatrix} \tag{2}$$

In (1), $M(q)$ is the symmetric inertia matrix, $N(q,\dot{q})$ is the matrix of centrifugal and Coriolis terms and $G(q)$ is the vector of torques produced by the gravitational force. In (2), τ_1 and τ_2 are the generalized forces corresponding to the generalized coordinates ψ and ϕ, respectively. In the present model, θ denotes the passive DOF and hence its corresponding generalized force is zero. The terms $M(q)$, $N(q,\dot{q})$ and $G(q)$ are defined as follows

$$M = [M_{ij}]_{3\times 3}, \quad N = [N_{ij}]_{3\times 3}, \quad G = [G_i]_{3\times 1} \tag{3}$$

where

$$\begin{aligned}
M_{11} &= I_t + I_{st} + I_{sw} \\
&\quad + m_t\left[d_t^2 + 2R(R + (d_t - R)\cos(\theta+\phi) - d_t)\right] \\
&\quad + m_{st}\left[d_{st}^2 + 2R(R + (d_{st} - R)\cos(\theta) - d_{st})\right] \\
&\quad + m_{sw}\left[d_{sw}^2 + 2R(R + (d_{sw} - R)\cos(\theta+\psi) - d_{sw})\right] \\
M_{12} &= I_t + m_t(d_t - R)(d_t - R + R\cos(\theta+\phi)) \\
M_{13} &= I_{sw} + m_{sw}(d_{sw} - R)(d_{sw} - R + R\cos(\theta+\psi)) \\
M_{22} &= I_t + m_t(d_t - R)^2 \\
M_{23} &= 0 \\
M_{33} &= I_{sw} + m_{sw}(d_{sw} - R)^2
\end{aligned}$$

$$
\begin{aligned}
N_{11} &= m_t R(R-d_t)\sin(\theta+\phi)(\dot\theta+\dot\phi) \\
&\quad + m_{st}R(R-d_{st})\sin(\theta)\dot\theta \\
&\quad + m_{sw}R(R-d_{sw})\sin(\theta+\psi)+(\dot\theta+\dot\psi) \\
N_{12} &= m_t R(R-d_t)\sin(\theta+\phi)(\dot\theta+\dot\phi) \\
N_{13} &= m_{sw}R(R-d_{sw})\sin(\theta+\psi)(\dot\theta+\dot\psi) \\
N_{21} &= N_{22} = N_{23} = 0 \\
N_{31} &= N_{32} = N_{33} = 0 \\
G_1 &= [m_t(R-d_t)\sin(\theta+\phi)+m_{st}(R-d_{st})\sin(\theta) \\
&\quad + m_{sw}(R-d_{sw})\sin(\theta+\psi)]\,g \\
G_2 &= m_t(R-d_t)\sin(\theta+\phi)\,g \\
G_3 &= m_{sw}(R-d_{sw})\sin(\theta+\psi)\,g
\end{aligned} \tag{4}
$$

and m_t, m_{st} and m_{sw} are the masses of the torso, stance leg and swing leg; I_t, I_{st} and I_{sw} are the mass moments of inertia of the torso, stance leg and swing leg about their respective center of gravity; R is the radius of curvature of the feet; d_t, d_{st} and d_{sw} are the distance of the center of gravity of the torso, stance leg and swing leg as shown in Fig.2; and g is the acceleration due to gravity.

The biped described above has three DOFs with two control inputs τ_1 and τ_2. In line with our discussion in section II, we impose the following two constraints on the motion of the system:

$$
\begin{aligned}
&\mathscr{C}_1 : \psi = -2\theta \\
&\mathscr{C}_2 : \alpha = \alpha_d
\end{aligned} \tag{5}
$$

where α is the angle of the torso with respect to the vertical and is defined by the relation

$$
\alpha = \phi + \theta - \pi \tag{6}
$$

and α_d is a constant. The constraint $\mathscr{C}_1$ ensures that the swing leg is always symmetric with respect to the stance leg about the vertical[3]. The constraint $\mathscr{C}_2$ ensures that the torso maintains angle α_d with respect to the vertical. The torques (τ_1 and τ_2) required to impose these constraints can be easily computed from (1). The constrained system has one passive DOF with the following dynamics[4], which is derived from (1)

$$
M_c(\theta)\,\ddot\theta + N_c(\theta,\dot\theta) + G_c(\theta) = 0 \tag{7}
$$

where

$$
\begin{aligned}
M_c &= I_{st} - I_{sw} + m_{st}d_{st}^2 - m_{sw}d_{sw}^2 \\
&\quad + (m_t+2m_{st})R^2 - 2R(m_{st}d_{st} - m_{sw}d_{sw}) \\
&\quad + m_t R(R-d_t)\cos\alpha_d - 2m_{st}R(R-d_{st})\cos\theta \\
N_c &= R\,[R(m_{st}-m_{sw}) - m_{st}d_{st} + m_{sw}d_{sw}]\sin\theta\,\dot\theta^2 \\
G_c &= [R(m_{st}-m_{sw}) - m_{st}d_{st} + m_{sw}d_{sw}]\,g \\
&\quad - m_t(R-d_t)\sin\alpha_d\; g
\end{aligned} \tag{8}
$$

For any set of reasonable parameter values, it can be verified that the biped described by (7) will have positive acceleration $\ddot\theta$ for positive angle α_d, and vice versa. In reality, however, the magnitude of $\dot\theta$ will not grow unbounded but reach a maximum due to friction and damping effects that have not been modeled.

[3]An additional DOF is required to ensure that the swing leg does not collide with the ground. A prismatic joint is used to provide this clearance in our experimental hardware. The dynamics of the prismatic joint is not significant and is therefore neglected in the present analysis.

[4]These dynamics are referred to as the zero dynamics [27] of the system.

IV. CONTROL DESIGN

The synthetic wheel biped rolls on its stance leg if the constraints in (5) are satisfied. When the point of contact with the ground reaches the toe of the stance leg during forward motion, or heel of the stance leg during backward motion, the stance and swing legs can be interchanged such that the biped can walk by rolling alternately on its two feet. In this section we present our control design for imposing the two constraints in (5). To this end, we first define the new set of generalized coordinates

$$
\bar q = \begin{bmatrix} \theta \\ v_1 \\ v_2 \end{bmatrix}, \qquad \begin{aligned} v_1 &= \alpha - \alpha_d \\ v_2 &= 2\theta + \psi \end{aligned} \tag{9}
$$

where α_d is the desired value of the angle of the torso with the vertical. The original generalized coordinates ψ and ϕ are related to the new coordinates v_1 and v_2 according to the following relations, which can be derived from (9)

$$
\begin{aligned}
\psi &= v_1 - \theta + \pi + \alpha_d \\
\phi &= v_2 - 2\theta
\end{aligned} \tag{10}
$$

Substituting (10) into (1), we obtain the dynamics of the system in terms of the new generalized coordinates as follows

$$
\bar M(\bar q)\,\ddot{\bar q} + \bar N(\bar q,\dot{\bar q})\,\dot{\bar q} + \bar G(\bar q) = T \tag{11}
$$

where $\bar M$, $\bar N$ and $\bar G$ have the same dimensions of M, N and G, respectively, and

$$
\begin{aligned}
\bar M_{11} &= I_{st} - I_{sw} + d_{st}^2 m_{st} - d_{sw}^2 m_{sw} - 2d_{st}m_{st}R \\
&\quad + 2d_{sw}m_{sw}R + (m_t+2m_{st})R^2 + 2m_{st}(d_{st}-R)R\cos(\theta) \\
&\quad + m_t R(-d_t+R)\cos(\alpha_d+v1) \\
\bar M_{12} &= I_t + m_t(d_t-R)^2 + m_t R(-d_t+R)\cos(\alpha_d+v_1) \\
\bar M_{13} &= I_{sw} + m_{sw}(d_{sw}-R)^2 + m_{sw}(d_{sw}-R)R\cos(\theta-v_2) \\
\bar M_{21} &= m_t R(-d_t+R)\cos(\alpha_d+v_1) \\
\bar M_{22} &= I_t + m_t(d_t-R)^2 \\
\bar M_{23} &= \bar M_{32} = 0 \\
\bar M_{31} &= -I_{sw} - m_{sw}(d_{sw}-R)^2 + m_{sw}(d_{sw}-R)R\cos(\theta-v_2) \\
\bar M_{33} &= I_{sw} + m_{sw}(d_{sw}-R)^2 \\
\bar N_{11} &= -2m_{sw}(d_{sw}-R)R\dot v_2\sin(\theta-v_2) \\
&\quad + \dot\theta(m_{st}R(-d_{st}+R)\sin(\theta) + m_{sw}(d_{sw}-R)R\sin(\theta-v_2)) \\
\bar N_{12} &= m_t(d_t-R)R\dot v_1\sin(\alpha_d+v_1) \\
\bar N_{13} &= m_{sw}(d_{sw}-R)R\dot v_2\sin(\theta-v_2) \\
\bar N_{21} &= N_{22} = N_{23} = 0 \\
\bar N_{31} &= N_{32} = N_{33} = 0
\end{aligned}
$$

$$
\begin{aligned}
\bar{G}_1 &= -d_{st} m_{st} \sin(\theta) + m_{st} R \sin(\theta) \\
&\quad + d_t m_t \sin(\alpha_d + v_1) - m_t R \sin(\alpha_d + v_1) \\
&\quad + d_{sw} m_{sw} \sin(\theta - v_2) - m_{sw} R \sin(\theta - v_2) \\
\bar{G}_2 &= d_t m_t \sin(\alpha_d + v_1) - m_t R \sin(\alpha_d + v_1) \\
\bar{G}_3 &= d_{sw} m_{sw} \sin(\theta - v_2) - m_{sw} R \sin(\theta - v_2)
\end{aligned} \tag{12}
$$

The generalized force corresponding to θ in Eq. (11) is zero and this allows the elimination of $\ddot{\theta}$ from the two equations corresponding to the generalized coordinates v_1 and v_2. The reduced-order equations have the form

$$
\hat{M}(\bar{q})\,\ddot{\hat{q}} + \hat{N}(\bar{q}, \dot{\bar{q}})\,\dot{\hat{q}} + \hat{G}(\bar{q}) = \hat{T} \tag{13}
$$

where $\hat{M} \in R^{2\times 2}$, $\hat{N} \in R^{2\times 2}$ and $\hat{G} \in R^{2\times 1}$ are functions of all three generalized coordinates θ, v_1 and v_2, and

$$
\hat{q} = \begin{bmatrix} v_1 \\ v_2 \end{bmatrix}, \qquad \hat{T} = \begin{bmatrix} \tau_1 \\ \tau_2 \end{bmatrix} \tag{14}
$$

Eq. (13) represents a completely actuated system and we use feedback linearization to design our controller as follows

$$
\hat{T} = \hat{N}(\bar{q}, \dot{\bar{q}})\,\dot{\hat{q}} + \hat{G}(\bar{q}) - \hat{M}(\bar{q})(K_d\,\dot{\hat{q}} + K_p\,\hat{q}) \tag{15}
$$

where K_d and K_p are diagonal positive-definite matrices of dimension two. Indeed, substitution of (15) into (13) results in

$$
\ddot{\hat{q}} + K_d\,\dot{\hat{q}} + K_p\,\hat{q} = 0 \tag{16}
$$

which implies $\hat{q} \to 0$ as $t \to \infty$. From the relations in (14) and (9) it simply follows that

$$
\alpha \to \alpha_d, \qquad \psi \to -2\theta \tag{17}
$$

as $t \to \infty$, *i.e.*, the constraints in (5) are satisfied.

Eq. (17) describes the behavior of two of the three DOF of the biped as it rolls on its stance leg. The behavior of the third DOF, namely θ, depends on the choice of α_d - it will have a positive acceleration for positive α_d and negative acceleration for negative α_d. This follows from our discussion in section III where friction and damping terms were not modeled. In reality, θ will accelerate and reach a maximum velocity due to friction and damping effects. The value of θ will however remain bounded at all times since it will be reset each time the stance and swing legs are interchanged.

The stability of the biped can be studied from the evolution of the states v_1 and v_2. These states are continuous during the interchange of the feet and therefore it can be shown that the synthetic wheel biped is a hybrid system with an asymptotically stable subsystem of dimension two, the proof of which is omitted for brevity.

In section III we derived the equations of motion of our biped using generalized coordinates that were convenient. The nonzero generalized forces corresponding to these coordinates, τ_1 and τ_2, are however different from those in our experimental hardware. In our biped platform, two actuators are placed at the hip: one controls the angle between the torso and the stance leg and the other controls the angle between the torso and the swing leg. We denote the torques produced by these actuators as τ_{st} and τ_{sw} and the corresponding generalized coordinates as γ_{st} and γ_{sw}. The angles α, γ_{st} and γ_{sw} form a complete set of generalized coordinates and are related to the coordinates in section III by the following forward and inverse relations

$$
\begin{aligned}
\alpha &= \theta + \phi - \pi & & \theta = \alpha + \gamma_{st} \\
\gamma_{st} &= \pi - \phi & \Rightarrow \quad & \phi = \pi - \gamma_{st} \\
\gamma_{sw} &= \pi - \phi + \psi & & \psi = \gamma_{sw} - \gamma_{st}
\end{aligned} \tag{18}
$$

Since the virtual work [28] is the same in both coordinates, we can write

$$
\tau_{st}\,\delta\gamma_{st} + \tau_{sw}\,\delta\gamma_{sw} = \tau_1\,\delta\phi + \tau_2\,\delta\psi \tag{19}
$$

On the other hand, we get from (18)

$$
\begin{aligned}
\delta\phi &= -\delta\gamma_{st} \\
\delta\psi &= \delta\gamma_{sw} - \delta\gamma_{st}
\end{aligned} \tag{20}
$$

Substitution of (20) into (19) gives

$$
\tau_{st} = -(\tau_1 + \tau_2), \qquad \tau_{sw} = \tau_2 \tag{21}
$$

Equations (15) and (21) together determine the torques to be applied by the motors in our biped platform for satisfying the constraints in (5).

V. EXPERIMENTS

A. Hardware Description

We designed and fabricated our synthetic wheel biped based on the schematic in Fig.2 but used paired legs to avoid lateral instability (see Fig.3). The inner paired leg has a fixed length but the outer paired leg has prismatic joints that increase leg length in the stance phase and and decrease leg length in the swing phase. The prismatic joints are not used for propulsion; their sole purpose is to provide foot clearance to the swing leg. In the vertically upright configuration, with both legs on the ground, the biped stands 1.09 *m* tall. The main structural material of the biped is 6061 Aluminum. The kinematic and dynamic parameters of the biped are provided in Table I.

Fig. 3. The synthetic wheel biped developed at Michigan State University

TABLE I

KINEMATIC AND DYNAMIC PARAMETERS OF SYNTHETIC WHEEL BIPED

Kinematic parameters			
	Length (m)	Foot radius, R (m)	Foot arc, β (deg)
Inner leg	0.635	0.635	22.5
Outer leg	0.635	0.635	22.5
Torso	0.457	-	-
Dynamic parameters			
	Mass (kg)	Inertia (kgm^2)	d in Fig.2 (m)
Inner leg	1.64	0.094	0.285
Outer leg	3.64	0.128	0.355
Torso	11.87	0.198	0.307

The robot has four 24 Volt DC servo motors: two of them (Maxon RE40, 150W) are located at the hip and control the angle of the stance leg and swing leg with respect to the torso; the other two (Faulhaber 3243 CR, 26.3W) provide simultaneous extension and contraction of the outer paired legs. Each hip drive is connected between the torso and a leg through a 43:1 planetary gearhead (Maxon 42C) and a final 2:1 helical gear drive. The leg extension motors have a 3.71:1 planetary gearhead (Faulhaber 38/1) and are connected to the bottom part of the leg through a 4.72 turn/cm ACME screw drive. The leg extensions ride on linear bearings for a smooth action.

The motors are driven by 4 digital motor drives (DZRALTE) donated by Advanced Motion Controls of Camarillo, CA. The hip joint drives are programmed to operate in current-control mode, requiring a +/-10 Volt DC analog signal proportional to the desired current or torque. The leg extension motors are run in a position control mode, requiring a +/-10 Volt DC analog signal proportional to the desired position.

Our biped relies on accurate absolute angle measurement of the torso to operate. To measure this, we have used one axis of an Intersense Inertiacube2+ 3D inertial sensor. This can provide torso angle data with an angular resolution of 0.01 degrees at a rate of 180 Hz. All of the motors have 500 count per turn optical incremental encoders (Agilent HEDS-5500) for position measurement. To simplify hip angle measurement, we have added encoder counter chips (Avago HCTL-2017) to the hip encoders. These allow our robot to easily determine the absolute position of the legs through the use of digital inputs on our data acquisition board.

The robot is controlled using a 12 Watt embedded computer (Winsystems EBC-855) running a C program on a Linux operating system. Data acquisition is provided through a PC104 format data acquisition board (PCM-MIO), also made by Winsystems. This system is capable of reading all of the sensors that we need while providing plenty of computational overhead, 802.11g wireless and Ethernet connectivity.

B. Experimental Results

The synthetic wheel biped in Fig.3 has no preferential direction of motion. With reference to Fig.2, it can walk in the direction of the positive x axis as well as negative x axis. To make the biped walk in the direction of the negative x axis, the desired angle of the torso with respect to the vertical was set to a negative value, equal to $\alpha_d = -1.5$ degrees. Since the torso has a large mass ($\approx 70\%$ of total mass - see Table I), a small torso angle is sufficient to cause the biped to walk. The biped was programmed to walk with the maximum step size. Since the biped was walking in the direction of the negative x axis, the stance and swing legs were interchanged when the point of contact of the stance leg with the ground reached the heel, *i.e.*, when $\theta = -\beta/2 = -11.25$ degrees (see Table I).

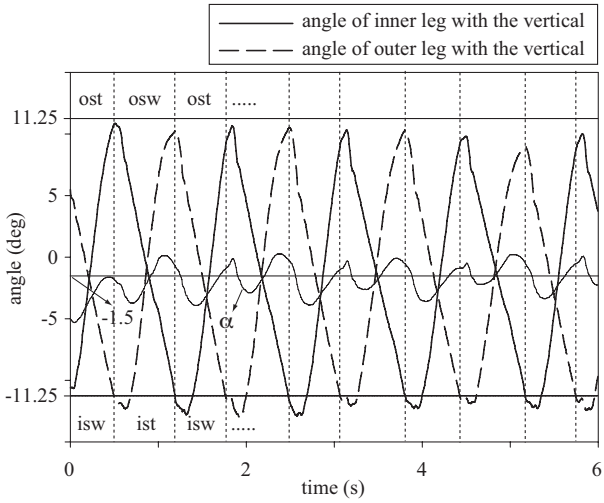

Fig. 4. Plots of angles subtended by the torso and the inner and outer legs with respect to the vertical.

The experimental results are shown in Fig.4 for arbitrary initial conditions. This figure has three plots. One of the plots show the variation in α with time. This plot indicates that α oscillates around the desired value of α_d with a small amplitude of approximately 2 degrees. The other two plots show the angle of the legs with respect to vertical while the vertical dotted lines indicate the times when stance and swing legs are interchanged. In the first time interval, the outer leg is the stance leg (ost) and the inner leg is the swing leg (isw). After the first interchange, the outer leg becomes the swing leg (osw) and the inner leg becomes the stance leg (ist). The plots of the leg angles show a small error in the positions of the swing leg at the time of switching as well as a small error in achieving a symmetric gait. These errors can come from the non-linear unmodeled dynamics of the system, limitations in applying high torques on the system, as well as the ignored dynamics of the prismatic joints.

The total power required to walk at $0.45m/s$ averages $55.4W$, corresponding to a total specific cost of transport ($energy\ used/[weight * distance\ traveled]$, C_{et}) of 0.73. Total power was determined by measuring the battery voltage and amperage using a 0.2 ohm current resistor and external data acquisition system at 500 Hz. By subtracting the energy required to run our computers and controllers, we determined a mechanical energy efficiency (C_{mt}). The power required to run the motors while walking averages $26.6W$, corresponding

to a mechanical energy efficiency of 0.35. This also includes the energy required to run the prismatic joints, which are both inefficient mechanisms and driven using high gains without attention to energy consumption. The power consumption without the leg extension motors averages $13.4W$, corresponding to a cost of transport of 0.18. A comparison of the robot's energy consumption to a number of other robots as well as a human walking is shown in Table II.

A video of our biped robot walking down a corridor will be shown at the conference.

TABLE II
ENERGY CONSUMPTION OF BIPEDS

		C_{et}	C_{mt}
Robots[1]	MSU Synthetic Wheel Biped	0.73	0.35/0.18
	Asimo	3.2	1.6
	TU Delft Denise	5.3	0.08
	MIT Spring Flamingo	2.8	0.07
	Cornell Collins 3D	0.20	0.055
	McGeer Dynamite	-	0.04
Humans	Walking	0.2	0.05

[1] Values found in [23] and [29]

VI. CONCLUSIONS

In this paper, we presented the control and design of a three-link underactuated synthetic wheel biped. Our design is based on the concept of a self-propelled wheel which enables the biped to walk forward and backward while avoiding impact during step transition. A controller based on feedback linearization was implemented on the biped. Experimental results show relatively good trajectory tracking leading to a stable gait with low mechanical cost of transport. Our future work will establish stability of the hybrid system described by the biped robot and focus on mechanical design and trajectory optimization for an energy efficient gait.

VII. ACKNOWLEDGMENTS

The funding provided by the National Science Foundation, NSF Grant CMMI 0925055, is appreciated. The authors would also like to thank Rene Ymzon of Advanced Motion Controls, Camarillo, CA, for donating the motor drives.

REFERENCES

[1] H. Lim and A. Takanishi, "Biped walking robots created at Waseda university: WL and Wabian family," *Philosophical Transactions of the Royal Society A: Mathematical, Physical and Engineering Sciences*, vol. 365, pp. 49–64, 2007.

[2] A. Takanishi, M. Ishida, Y. Yamazaki, and I. Kato, "The realization of dynamic walking by the biped walking robot," in *IEEE International Conference on Robotics and Automation*, 1985, pp. 459–466.

[3] M. Vukobratovic and D. Juricic, "Contribution to synthesis of biped gait," *IEEE Transactions on Biomedical Engineering*, vol. BM16, no. 1, pp. 1–6, 1969.

[4] A. Goswami, "Postural stability of biped robots and the foot-rotation indicator (FRI) point," *International Journal of Robotics Research*, vol. 18, no. 6, pp. 523–533, 1999.

[5] P. Sardain and G. Bessonnet, "Forces acting on a biped robot: Center of pressure-zero moment point," *IEEE Transactions on Systems Man and Cybernetics, Part A - Systems and Humans*, vol. 34, no. 5, pp. 630–637, 2004.

[6] M. Vukobratovic, B. Borovac, and V. Potkonjak, "ZMP: A review of some basic misunderstandings," *International Journal of Robotics Research*, vol. 3, no. 2, pp. 153–175, 2006.

[7] P. Sardain, H. Rostami, and G. Bessonnet, "An anthropomorphic biped robot: Dynamic concepts and technological design," *IEEE Transactions on Systems Man and Cybernetics, Part A - Systems and Humans*, vol. 28, no. 6, pp. 823–838, 1998.

[8] H. Hirukawa, F. Kanehiro, K. Kaneko, S. Kajita, K. Fujiwara, Y. Kawai, F. Tomita, S. Hirai, K. Tanie, T. Isozumi, K. Akachi, T. Kawasaki, S. Ota, K. Yokoyama, H. Handa, Y. Fukase, J. Maeda, Y. Nakamura, S. Tachi, and H. Inoue, "Humanoid robotics platforms developed in HRP," *Robotics and Autonomous Systems*, vol. 48, pp. 165–175, 2004.

[9] I.-W. Park, J.-W. Kim, J. Lee, and J.-H. Oh, "Mechanical design of the humanoid robot platform, HUBO," *Advanced Robotics*, vol. 21, no. 11, pp. 1305–1322, 2007.

[10] Y. Sakagami, R. Watanabe, C. Aoyama, S. Matsunaga, N. Higaki, and K. Fujimura, "The intelligent Asimo: System overview and integration," in *IEEE/RSJ International Conference on Intelligent Robots and Systems*, vol. 3, 2002, pp. 2478–2483.

[11] M. Hirose and K. Ogawa, "Honda humanoid robotics development," *Philosophical Transactions of the Royal Society A: Mathematical, Physical and Engineering Sciences*, vol. 365, pp. 11–19, 2007.

[12] C. Chevallereau, G. Abba, Y. Aoustin, F. Plestan, E. Westervelt, C. C. de Wit, and J. Grizzle, "Rabbit: A testbed for advanced control theory," *IEEE Control Systems Magazine*, vol. 23, pp. 57–79, 2003.

[13] E. Westervelt, J. Grizzle, and D. Koditschek, "Hybrid zero dynamics of planar biped walkers," *IEEE Trans. on Automatic Control*, vol. 48, pp. 42–56, 2003.

[14] S. Kawaji, K. Ogasawara, J. Iimori, and S. Yamada, "Compliance control for biped locomotion robot," in *IEEE International Conference on Systems, Man, and Cybernetics*, vol. 4, 1997, pp. 3801–3806.

[15] J. Park, "Impedance control for biped robot locomotion," *IEEE Transactions on Robotics and Automation*, vol. 17, no. 6, pp. 870–882, 2001.

[16] M. H. Raibert, *Legged Robots that Balance*. Cambridge, MA, USA: Massachusetts Institute of Technology, 1986.

[17] G. Pratt, "Low impedance walking robots," *Integrative and Comparative Biology*, vol. 42, no. 1, pp. 174–181.

[18] J. Yamaguchi, D. Nishino, and A. Takanishi, "Realization of dynamic biped walking varying joint stiffness using antagonistic driven joints," *IEEE International Conference on Robotics and Automation*, vol. 3, pp. 2022–2029, 1998.

[19] B. Vanderborght, "Dynamic stabilisation of the biped Lucy powered by actuators with controllable stiffness," Ph.D. dissertation, Vrije University, Brussels, 2007.

[20] T. McGeer, "Passive dynamic walking," *The International Journal of Robotics Research*, vol. 9, no. 2, pp. 62–82, 1990.

[21] D. G. E. Hobbelen and M. Wisse, "A disturbance rejection measure for limit cycle walkers: The gait sensitivity norm," *IEEE Transactions on Robotics*, vol. 23, no. 6, pp. 1213–1224, 2007.

[22] M. Wisse, G. Feliksdal, J. V. Frankenhuyzen, and B. Moyer, "Passive-based walking robot - Denise, a simple effiient and lightweight biped," *IEEE Robotics and Automation Magazine*, vol. 14, no. 2, pp. 52–62, 2007.

[23] S. Collins, M. Wisse, and A. Ruina, "A three-dimensional passive-dynamic walking robot with two legs and knees," *The International Journal of Robotics Research*, vol. 20, no. 7, pp. 607–615, 2001.

[24] Y. Ikemata, A. Sano, and H. Fujimoto, "A physical principle of gait generation and its stabilization derived from mechanism of fixed point," *IEEE International Conference on Robotics and Automation*, pp. 836–841, May 2006.

[25] M. Wisse, D. G. E. Hobbelen, and A. L. Schwab, "Adding an upper body to passive dynamic walking robots by means of a bisecting hip mechanism," *IEEE Transactions on Robotics*, vol. 23, no. 1, pp. 112–123, 2007.

[26] T. Das and R. Mukherjee, "Dynamic analysis of rectilinear motion of a self-propelling disk with unbalance masses," *Journal of Applied Mechanics*, vol. 68, no. 1, pp. 58–66, 2001.

[27] H. K. Khalil, *Nonlinear Systems*, 3rd ed. Prentice Hall, 2002.

[28] D. T. Greenwood, *Principles of Dynamics*, 2nd ed. Prentice Hall, 1988.

[29] S. Collins and A. Ruina, "A bipedal walking robot with efficient and human-like gait," in *IEEE International Conference on Robotics and Automation*, 2005, pp. 1983–1988.